Biophysical Chemistry 21 (1985) 295–313
Elsevier

BPC 00917

DYNAMIC PROPERTY OF MEMBRANE FORMATION IN A PROTOPLASMIC DROPLET OF *NITELLA*

Kiyoshi TOKO, Masaaki NOSAKA, Masaru TSUKIJI and Kaoru YAMAFUJI

Department of Electronics, Faculty of Engineering, Kyushu University 36, Fukuoka 812, Japan

Received 31st July 1984
Revised manuscript received 10th September 1984
Accepted 5th November 1984

Key words: Nitella; Surface membrane; Protoplasmic droplet; Electrochemical study; Oscillation; Nonequilibrium thermodynamics

A theory is presented to explain the dynamic characteristics of an electric potential and the resistance of a surface membrane during the formation of a protoplasmic droplet isolated from *Nitella*. Basic equations are coupled ones for describing ion concentrations near the surface of the droplet, active and passive ion fluxes on the surface, and kinetics of membrane-constituting molecules diffusing from the inside of the protoplasm. The present results give a good explanation of the observed kinetics of electric properties throughout the formative process of surface membranes after the ion concentrations are replaced by lower ones. The results can also explain well the observed data on the steady state. Oscillatory changes in the membrane potential induced by ions strongly adsorbed on the surface membrane are discussed in relation to growth and regeneration phenomena in biological systems such as bean roots and *Acetabularia*.

1. Introduction

The process of membrane formation is an indispensable step in the growth of biological systems. A surface membrane formed on a protoplasmic droplet of *Nitella* develops into an excitable membrane when the external solution is exchanged for an aqueous solution with low ion concentrations [1], while it shows no excitability under high ion concentrations. It is suggested from physicochemical experiments [1] that micelles of phospholipids are loosely bound with each other in a depolarized state of the surface membrane showing no excitability. In a resting state of a surface membrane showing excitability, on the other hand, lipid-protein complexes are formed by penetration of proteins into the membrane which is formed by lipids.

Two kinds of aqueous solutions are chosen in usual experiments for examining the structural change in surface membranes [1]: one is called a basal solution with relatively high ion concentrations (70 mM KNO_3, 50 mM NaCl, 5 mM $CaCl_2$), and the other is a testing solution (0.5 mM KNO_3, 0.5 mM NaCl, 1 mM $Ca(NO_3)_2$, 2 mM $Mg(NO_3)_2$) with much lower ionic strength than that in the protoplasm. Since the excitability appears in the testing solution, the excitability of a membrane is retained only in the presence of strong ion fluxes across the surface, i.e., only in a far-from-equilibrium condition. If we note that molecules constituting the membrane are derived from the inside of the protoplasm by diffusion [2,3], the membrane-forming process can also be acknowledged as a typical self-organization process in a nonequilibrium open system. In fact, a repetition of disruption and formation of membrane is induced by addition of UO_2^{2+}, and gives rise to oscillations of the membrane potential and membrane resistance [4].

The purpose of the present paper is to explain theoretically these dynamic properties of the membrane in a nonequilibrium open system on the basis of our previous electrochemical studies [3,5]. In these studies, it was shown that the surface

membrane regarded as a kind of adsorbed bilayer is formed, resulting in the inhomogeneous distribution of lipid and protein molecules at the surface through a Ca^{2+}-bridging ability. Observed data on the steady-state characteristics were explained quantitatively; a competitive relationship between monovalent cations and Ca^{2+} was shown to play an important role in the phase transition from the depolarized state to the resting state, while the dynamic features of membrane formation were not investigated. Although the kinetics of formation of excitable membranes was also discussed in a general fashion with kinetic equations containing phenomenological coefficients from the viewpoint of nonequilibrium thermodynamics [2], detailed electrochemical considerations were not presented.

The present paper is mainly devoted to an electrochemical description of the membrane-forming process after the replacement of the basal solution by the testing solution. Basic equations are coupled ones for ion concentrations near the surface inside the droplet, an activation of pump molecules at the surface and kinetics of membrane-constituting molecules. Dynamic changes in measured quantities such as the membrane potential and resistance are explained fairly well. It is shown that, once the membrane has been formed, the droplet recovers the original ion concentration so as to maintain a large ion-concentration gradient across the membrane. By taking into account the binding effect of UO_2^{2+} on the membrane, periodic changes in the membrane potential and resistance are shown to occur according to disruption and formation of the membrane. The relation between membrane formation and rather macroscopic processes and as growth and regeneration is also discussed.

2. Phase transition between resting and depolarized states

We mention a theoretical procedure for describing steady-state characteristics of the phase transition between resting and depolarized states [3]. A slight modification and simplification are made in discussing the dynamic properties of membrane formation; this will be given in the next section.

2.1. Total free energy of a protoplasmic droplet

Fig. 1 shows a theoretical model of a protoplasmic droplet in an external solution. The droplet is composed of a surface membrane, an inner surface region and a central region.

Since lipids and proteins constituting the surface membrane of a protoplasmic droplet are derived from the inside of the protoplasm by diffusion [2], the resultant membrane can be regarded as a kind of adsorbed bilayer. The adsorbed bilayer in the resting state is composed of lipid-protein complexes formed by the accumulation of lipids and subsequent penetration of proteins. The bilayer in the depolarized state consists of loosely bound lipids [1]. Thus, the depolarized and resting states

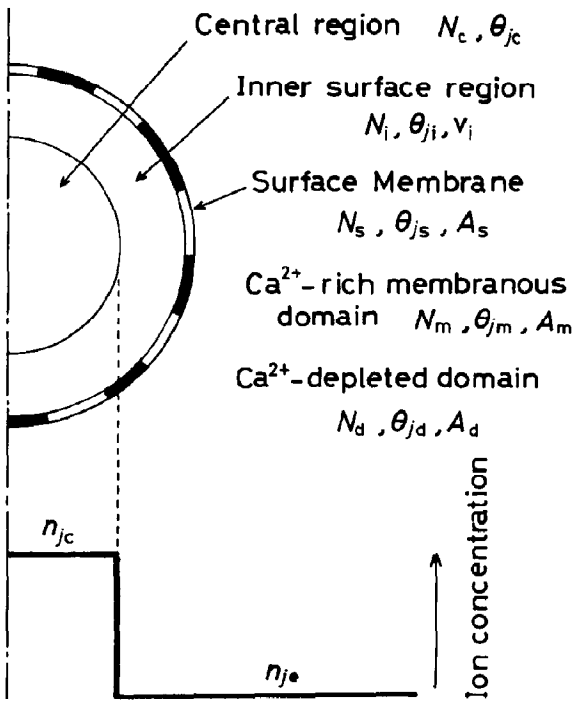

Fig. 1. A simplified theoretical model [3]. A surface membrane is composed of Ca^{2+}-rich membranous and Ca^{2+}-depleted domains, which are denoted by dark and bright regions, respectively. The membrane is a kind of adsorbed bilayer constructed by proteins and lipids diffusing from the inner surface region. Divalent cations such as Ca^{2+} are bound to the membrane for the most part, leading to the phase-separation state.

can be characterized respectively by lower and higher packing densities of adsorbed molecules. The observed tendencies in the phase transition between resting and depolarized states can be sufficiently described by the average packing density as a function of external ion concentrations. Therefore, we do not consider or specify differences among various species of molecules such as lipids and proteins contained in the droplet.

The surface membrane in the depolarized state appearing in a basal solution is highly permeable to ions. It can be seen from a low electric resistance and nearly zero membrane potential [1]. When the external solution is replaced by a testing solution with much lower ion concentrations than in the protoplasm, the ion concentration in the protoplasm should vary continuously from the central region. However, a noticeable change in the ion concentration is expected to occur only near the surface of the droplet, and hence we can divide the whole region inside the droplet into two regions: one is the central region where the ion-concentration change is negligible, the other being the inner region near the surface. We call the latter region the inner surface region, and furthermore neglect the transitional region between the central and inner surface regions by approximately assuming the ion concentration in each region as uniform, for simplicity. In addition, we regard the ion concentration in the inner surface region as being equal to the external ion concentration. the restriction will be relaxed in the following section by taking into account active and passive ion fluxes on the droplet surface (see fig. 5).

Let us define here some quantities in each region and the surrounding aqueous phase in fig. 1: N_c, N_i, N_s, N_m, N_d, number of lipids and proteins; θ_{jc}, θ_{ji}, θ_{js}, θ_{jm}, θ_{jd}, degree of adsorption of j-th cations on lipids and proteins; A_s, A_m, A_d, surface area; n_{jc}, n_{je}, concentration of j-th cations; v_i, volume of the inner surface region.

The parameters which can be controlled experimentally are the external ion concentrations n_{je}. We regard the surface membrane as being composed of two interacting adsorbed monolayers. The condition of the ion concentration in the inner surface region being equal to the external one leads to indistinguishable electrochemical properties of these two monolayers. Therefore, the quantities concerned with each monolayer N_s, N_m, N_d, A_s, A_m and A_d should be simple multiplied by a factor of two, when the quantities concerned with the surface membrane are needed. This simplification is no longer valid if the ion concentration in the inner surface region differs from the external ion concentration, as will be shown in the subsequent section.

Let us denote the total number of lipids and proteins contained in a droplet by N_T; then the following relation exists for a fixed value of N_T:

$$2N_s + N_i + N_c = N_T. \tag{1}$$

To explain the phase transition between resting and depolarized states, we assume that a phase separation occurs between two domains on the surface membrane due to the bridging among adsorbed molecules through Ca^{2+}; one is the Ca^{2+}-rich membranous domain, where adsorbed molecules are packed tightly due to the Ca^{2+}-bridging to form a membrane structure, the other being the Ca^{2+}-depleted domain composed of sparsely distributed molecules. The quantities concerned with the surface membrane have the relations:

$$\begin{aligned} &N_m + N_d = N_s, \\ &A_m + A_d = A_s, \\ &N_m\theta_{jm} + N_d\theta_{jd} = N_s\theta_{js}, \end{aligned} \tag{2}$$

where the subscript s represents the surface, and A_s designates the total surface area of the protoplasmic droplet concerned, which may be considered as constant.

We must here explain the etymology of Ca^{2+}-rich membranous domain. As seen later (cf. table 1), an excitable surface membrane which is hardly permeable to ions can be formed in the resting state when this domain is dominant. To emphasize the membrane structure mainly formed by this domain in the resting state, we call this domain the Ca^{2+}-rich membranous domain. Furthermore, the subscript m added in A_m, N_m and θ_{jm} implies not only 'membranous' but also 'micelles of lipids' because A_m becomes equal to A_s when the phase separation disappears at high ion concentrations so as to result in the appearance of the depolarized state, where micelles of lipids occupy the dominant phase.

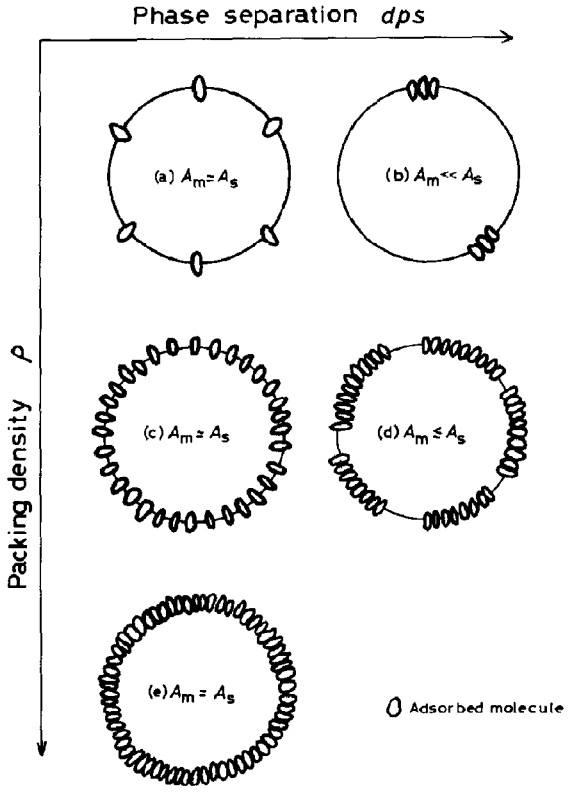

Fig. 2. Schematic illustration of the lateral configurations of adsorbed molecules at the surface of protoplasmic droplets.

In the present model, the state of a homogeneous distribution without phase separations is assumed to be realized when N_m, A_m and θ_{jm} approach N_s, A_s and θ_{js}, respectively. As one of the convenient ways to express the criterion as to whether the phase separation occurs, let us introduce a degree of phase separation (dps) by

$$\mathrm{dps} = 1 - (A_m/A_s). \tag{3}$$

Eq. 3 shows that dps takes values from zero to unity and approaches zero when the phase separation disappears. When the value of A_m resulting from the minimization of the total free energy is substituted into eq. 3, therefore, dps can be regarded as a kind of order parameter which expresses the lateral configuration of adsorbed molecules on the surface membrane. As will be mentioned, dps takes a value of about zero in the depolarized state observed in high ion concentrations. It implies that A_m in this depolarized state equals the surface area of droplet, A_s, on which micelles of phospholipids distribute homogeneously and are loosely bound with each other. Fig. 2 demonstrates the possible lateral configuration of adsorbed molecules when the phase separation is taken into account, where ρ is the packing density defined by eq. 10.

Now we can write a formal expression for the free energy of the present system, F, in k_BT units (k_B, Boltzmann's constant; T, absolute temperature) as

$$\begin{aligned} F = {} & 2N_m(f_{0,m} + f_{el,m} + \epsilon_{ch,m}) \\ & + 2N_d(f_{0,d} + f_{el,d} + \epsilon_{ch,d}) \\ & + E_b + N_i(f_{0,i} + f_{el,i}) + N_c(f_{0,c} + f_{el,c}) \\ & + [2N_m \ln(2N_m) + 2N_d \ln(2N_d) \\ & + N_i \ln N_i + N_c \ln N_c]. \end{aligned} \tag{4}$$

In eq. 4, subscripts 0, el, ch and b designate nonelectric, electrochemical, changeable bridging and boundary energies, respectively. The first term in parentheses in eq. 4 corresponds to the free energy of adsorbed molecules in the Ca^{2+}-rich membranous domains, and the second is the energy in the Ca^{2+}-depleted domains. The third term designates a boundary energy between these domains. The fourth term represents the free energy of molecules in the inner surface region, the fifth term being that in the central region. The sixth term is the mixing entropy originating from the mixing of the above two domains and two regions.

2.2. Simplification of the total free energy

Since eq. 4 contains too many internal variables to be handled analytically, we try to reduce the number of internal variables.

2.2.1. Approximations of the number of lipids and proteins

First, let us assume that N_c is constant in the present model. Then, the total number of lipids and proteins N contained in the surface membrane and inner surface region remains unchanged:

$$2N_s + N_i = N_T - N_c = N = \text{constant} \tag{5}$$

Second, we make the approximation that N_d is much smaller than N_m, because the packing density in Ca^{2+}-depleted domains may be much smaller than that in Ca^{2+}-rich membranous domains. Eq. 2 leads to

$$N_m = N_s. \tag{6}$$

Note that N_d and A_m are independent internal variables, irrespective of the above approximation. Since the degree of phase separation is defined by eq. 3, the present approximation does not contradict our starting assumption on the occurrence of phase separation.

From these approximations, the free energy F of eq. 4 is reduced to the much simpler form:

$$F = F_0 + F_{el} + E_{ch} + E_b; \tag{7}$$

$$F_0 = 2N_s f_{0,m} + (N - 2N_s) f_{0,i} + 2N_s \ln(2N_s) + (N - 2N_s) \ln(N - 2N_s),$$

$$F_{el} = 2N_s f_{el,m} + (N - 2N_s) f_{el,i},$$

$$E_{ch} = 2N_s \epsilon_{ch,m}, \tag{8}$$

where F_0 represents the nonelectric energy and F_{el} is the electrochemical energy. The third term in eq. 7 is the changeable part of the bridging energy [5], the final one being the boundary energy. To give an explicit expression for each term in eq. 7 needs further approximations.

2.2.2. Approximations of the adsorption of cations on lipids and proteins

First, let us neglect the adsorption of monovalent cations such as Na^+ and K^+ on lipids and proteins, as has been usually done [6].

$$\theta_{1k} = 0 \quad \text{for k = i, m.} \tag{9}$$

Next, the effect of adsorption of Mg^{2+} can be disregarded, since Mg^{2+} binding is still weaker than Ca^{2+} binding, which is the case in phosphatidylglycerol monolayers [7] and other kinds of monolayers and bilayers [8]. Furthermore, Ca^{2+} can induce a phase separation in phosphatidylserine/phosphatidylcholine membranes but Mg^{2+} cannot [9]. In fact, Mg^{2+} is not indispensable for the maintenance of excitable membranes of *Nitella* [1]. For simplicity, we consider only the situation where Ca^{2+} is adsorbed on the monovalent negatively charged group of lipids and proteins.

To describe the phase transition in the droplet, let us express the energies in eq. 7 in terms of the packing density [10] defined by

$$\rho = N_s a / A_s, \tag{10}$$

where a represents the limiting area by one adsorbed molecule averaged over different species of molecules in the droplet. With eq. 6, ρ is approximated by

$$\rho = N_m a / A_s, \tag{11}$$

For the packing density in Ca^{2+}-rich membranous domains, let us define it as follows:

$$\rho_m = N_m a / A_m = N_s a / A_m. \tag{12}$$

The free energies of Ca^{2+}-rich membranous domains in eq. 7 can be expressed by means of ρ_m.

2.2.3. Approximation of the relation between A_m and N_s

As a result of the above approximations, the total free energy given by eq. 7 can be described as a function of four internal variables: A_m, N_s (= N_m), θ_{2m} and θ_{2i}. However, it is more convenient to express A_m in terms of N_s and the external monovalent and divalent cation concentrations, n_{1e} and n_{2e}, respectively. This can be done by an electrochemical consideration such as

$$A_m / A_s = u(N_s; n_{1e}, n_{2e}), \tag{13}$$

where the functional form is given by [3,5]

$$u = 1 - (1 - \rho^r) \exp[-q(n_{1e} + 3n_{2e})], \tag{14}$$

with q and r the numerical parameters. Then, ρ_m defined by eq. 12 is rewritten as

$$\rho_m = \rho / u. \tag{15}$$

Fig. 3 illustrates the relationship between ρ_m and ρ. The phase separation appears when the ionic strength is decreased, which leads to the local enhancement of packing density. Thus, ρ_m in Ca^{2+}-rich membranous domains is larger than ρ averaged over the surface membrane. For ρ close to unity, ρ_m must approach to unity.

2.3. Explicit expression for each part of the free energy

Let us now provide expressions for the nonelectric, electrochemical, changeable bridging and boundary energies appearing in eq. 7 as a function of three internal variables, N_s ($= N_m$), θ_{2m} and θ_i. Firstly, the nonelectric free energy in k_BT units, F_0, is given by

$$F_0 = 2N_s\left(-\epsilon_0 + \frac{\epsilon_r}{\gamma+1}\rho_m^{\gamma} - \frac{\epsilon_a}{\gamma'+1}\rho_m^{\gamma'} - \frac{\epsilon_h}{2}\rho_m\right) + 2N_s \ln\left[\frac{N_s}{\Delta l(A_m - N_s a)}\right] + (N - 2N_s)\ln\left[\frac{N-2N_s}{v_i}\right], \quad (16a)$$

neglecting trivial small terms. The parameters ϵ_0, ϵ_r, ϵ_a and ϵ_h refer to the nonelectric affinity potential of molecules adsorbed to the surface of a protoplasmic droplet, repulsive and van der Waals attractive interactions among adsorbed molecules, and the interaction between the opposite monolayers constituting the bilayer, respectively. Here the exponents γ and γ' are taken as $\gamma = 11/2$ and $\gamma' = 5/2$ [10]. In the entropy term in eq. 16a, Δl is the translational length of adsorbed molecules.

Secondly, the approximations of eqs. 9 and 12 give the electrochemical energy in k_BT units [3,5,6,11]:

$$F_{el} = 2N_s\left\{\int_{1/2}^{\theta_{2m}} \ln\left[\frac{1}{K_2 n_{2e}}\cdot\frac{2\theta}{1-2\theta}\right]d\theta + \left(\frac{a}{\rho_m k_B T}\right)\int_0^{\sigma}\psi(\sigma)d\sigma\right\} + (N-2N_s)\int_{1/2}^{\theta_{2i}} \ln\left[\frac{1}{K_2 n_{2e}}\cdot\frac{2\theta}{1-2\theta}\right]d\theta, \quad (16b)$$

where the average adsorption constant of Ca^{2+} is denoted by K_2, and ψ and σ designate the electrostatic potential at the surface and the surface charge density, respectively. The surface charge density σ is given by

$$\sigma = -N_s e(1-2\theta_{2m})/A_m = -(e\rho/au)(1-2\theta_{2m}), \quad (17)$$

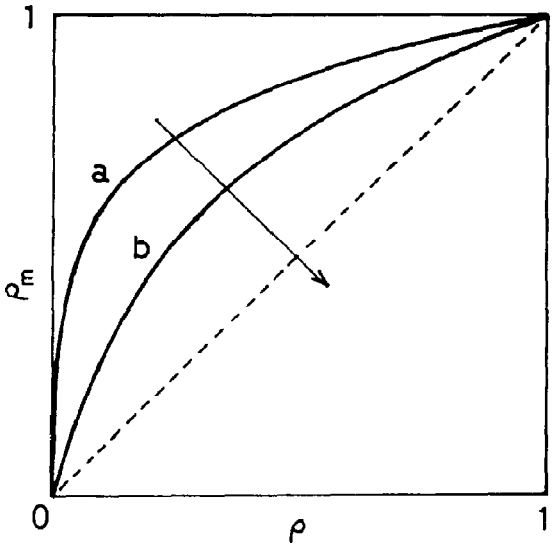

Fig. 3. Relation between ρ_m and ρ. Ionic strength: 0.1 mM for curve a and 5 mM for curve b. The increase in ionic strength makes ρ_m approach ρ, as shown by the arrow.

when e is the positive elementary charge. Integration of the Poisson-Boltzmann equation gives another expression for σ as a function of ion concentrations:

$$\sigma = \sqrt{2\epsilon_W k_B T/\pi} \times \sinh(\phi/2)\left[n_{1e} + n_{2e}(e^{-\phi}+2)\right]^{1/2}, \quad (18)$$

where ϵ_W is the dielectric permeability of water, and the reduced electrostatic potential at the surface ϕ is defined by

$$\phi = e\psi/k_BT. \quad (19)$$

Thirdly, the changeable part of the bridging energy depends explicitly on the surface area occupied by one molecule; hence, it may be of a form slightly modified from that used previously [5]:

$$E_{ch} = -2N_s\epsilon_2\theta_{2m}^2\sqrt{\rho_m}, \quad (16c)$$

where the parameter ϵ_2 represents the strength of the energy. The changeable bridging energy E_{ch} is enlarged by the increased degree of adsorption of Ca^{2+} and increased packing density.

Finally, the boundary energy may be of the form [5]:

$$E_b = 2N_s\tilde{\epsilon}_b\lambda^{-2}/\sqrt{u}\,. \tag{16d}$$

This expression contains one numerical coefficient $\tilde{\epsilon}_b$ as a measure of the increase in energy brought about by a neighboring contact of two domains [5,12]. A normalized and modified screening length, λ, is defined by

$$\lambda^{-2} = 1 + (8\pi e^2/\epsilon_W k_B T)a(n_{1e} + 3n_{2e}). \tag{20}$$

The decrease in λ accompanied by the increased ionic strength gives rise to an increase in the boundary energy. The sharp spatial variation of electric field is disadvantageous to the formation of neighboring domains.

2.4. Description of the steady-state characteristics

The total free energy F is given by eq. 7 with the explicit expressions, eqs. 16a–16d, where ρ_m is given by eq. 15 in terms of u and ρ. A set of equations for ρ (or ρ_m), θ_{2i} and θ_{2m} can be obtained by minimizing eq. 7 with respect to N_s, θ_{2i} and θ_{2m}. From the minimization with respect to θ_{2i} and θ_{2m}, the equations for degrees of adsorption become

$$1 - 2\theta_{2i} = (1 + K_2 n_{2e})^{-1}, \tag{21}$$

and

$$1 - 2\theta_{2m} = \left\{1 + K_2 n_{2e} \exp\left[-2\phi + 2\epsilon_2\theta_{2m}\sqrt{\rho/u}\right]\right\}^{-1}, \tag{22}$$

where ϕ is an implicit function of θ_{2m} through eqs. 17 and 18.

Next, the minimization with respect to N_s leads to

$$0 = \Delta g_0 + \Delta g_{el} + \Delta g_{ch} + \Delta g_b, \tag{23}$$

where Δg_0, etc., are the differentiation of the corresponding energies with respect to N_s, and are given by

$$\Delta g_0 = -(\epsilon_0 + \ln c) + \epsilon_r(\rho/u)^{\gamma} - \epsilon_a(\rho/u)^{\gamma'} - \epsilon_b(\rho/u) - \ln\{\Delta l a[(u/\rho) - 1]\} + (1 - P)/[(u/\rho) - 1] - P\left[\frac{\gamma}{\gamma + 1}\epsilon_r(\rho/u)^{\gamma+1} - \frac{\gamma'}{\gamma' + 1}\epsilon_a(\rho/u)^{\gamma'+1} - \frac{\epsilon_b}{2}(\rho/u)^2\right], \tag{24a}$$

$$\Delta g_{el} + \Delta g_{ch} = (1/2)\ln(\theta_{2m}/\theta_{2i}) - PaII_{el}/k_B T - \epsilon_2\theta_{2m}(1 - \theta_{2m}/2)\sqrt{\rho/u} + (P/2)\epsilon_2\theta_{2m}^2(\rho/u)^{3/2}, \tag{24b}$$

$$\Delta g_b = \tilde{\epsilon}_b\lambda^{-2}[1 - (P/2)(\rho/u)]/\sqrt{u}\,, \tag{24c}$$

with the definitions of c and P as follows:

$$c = N/v_i, \tag{25}$$

$$P = r\rho^{r-1}\exp[-q(n_{1e} + 3n_{2e})]. \tag{26}$$

In eq. 24b, II_{el} is the electrostatic pressure as a function of n_{1e}, n_{2e} and ϕ. The contribution of this term to $(\Delta g_{el} + \Delta g_{ch})$ is negligibly small. A detailed derivation and an explicit form as therefore omitted here (see refs. 3, 5, 7 and 13).

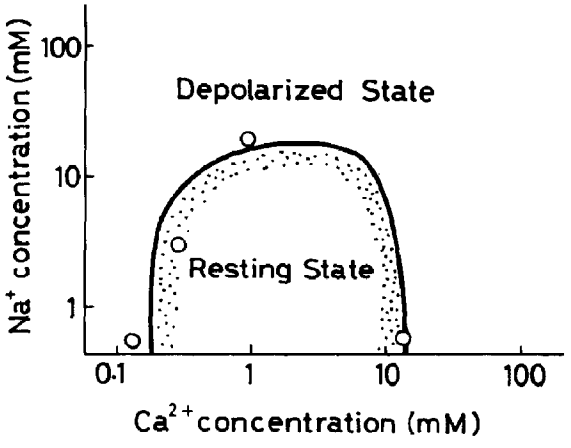

Fig. 4. Phase diagram as a function of Na^+ and Ca^{2+} concentrations. The solid line refers to the theory [3], and open circles denote the observed phase-transition points [1]. Ionic composition other than Na^+ and Ca^{2+} is fixed at 0.5 mM KNO_3 and 2 mM $Mg(NO_3)_2$. The effect of Mg^{2+} is taken into account by adding a concentration 3-times as large as the Mg^{2+} concentration to the external monovalent cation concentration. Parameters: $\epsilon_r = 8$, $\epsilon_1 = 13$, $\epsilon_b = 4$, $\Delta l = 1$ (Å), $a = 100$ (Å^2), $K_2 = 0.5$ (M^{-1}), $\epsilon_2 = 4$, $\tilde{\epsilon}_b = 5$, $r = 0.8$, $q = 47.25$ (M^{-1}), $\epsilon_0 + \ln c = 9$.

Table 1
Theoretical result on the states of the surface membrane of a protoplasmic droplet

	$[Na^+] \lesssim 20$ mM and $[Ca^{2+}] \lesssim 0.2$ mM	$[Na^+] \lesssim 20$ mM and 0.2 mM $\lesssim [Ca^{2+}] \lesssim 10$ mM	$[Na^+] \gtrsim 20$ mM or $[Ca^{2+}] \gtrsim 10$ mM
State	depolarized	resting	depolarized
Packing density ρ	≈ 0	≈ 0.8	≈ 0.05
Degree of phase separation dps	≈ 0.7	≈ 0.2	≈ 0
Illustration in fig. 2	b	d	a

The degree of adsorption θ_{2i} is given directly by eq. 21, and θ becomes a function of ρ by solving numerically an adsorption equilibrium constructed from eqs. 17, 18 and 22 for any value of n_{1e} and n_{2e}. The packing density ρ is calculated by substituting these values of θ_{2i}, θ_{2m} and ϕ into eq. 23 with eqs. 24. As a result, the phase transition between the resting and depolarized states in a protoplasmic droplet of *Nitella* is described for any change in ion concentrations.

Fig. 4 shows the theoretical result on a phase diagram of the *Nitella* protoplasmic droplet in the plane of Na^+ and Ca^{2+} concentrations. It surely explains the experimental observation that the resting state exists within a limited range of Na^+ and Ca^{2+} concentrations. Furthermore, fig. 4 demonstrates that the phase transition is subject to a competition between Na^+ and Ca^{2+} concentrations at lower ion concentrations, and an ionic strength factor at high ion concentrations.

The present theory is constructed so that a state of the phase separation between Ca^{2+}-rich membranous and Ca^{2+}-depleted domains due to the Ca^{2+} bridging can also be described (if it occurs). The result shows that phase separation does occur within some region of ion concentrations. Here, we give a qualitative description of the phase transition in a protoplasmic droplet of *Nitella*, pointing to the effect of Ca^{2+} bridging.

Table 1 summarizes the theoretical results on states of the surface membrane of a protoplasmic droplet: at very low ion concentrations, the present calculation gives $\rho \approx 0$ and $\rho/\rho_m = A_m/A_s \approx 0.3$ as typical values. Then the degree of phase separation dps $= 1 - (A_m/A_s)$ defined by eq. 3 yields a value of about 0.7. From the low value of ρ, the membrane can be regarded as being depolarized (see also fig. 8). This corresponds to case b in fig. 2.

An increase in Ca^{2+} concentration in a low Na^+ concentration leads to both a decrease in $|\psi|$ and an increase in θ_{2m}. The main terms in eq. 24b are the first and third ones, and hence the above-mentioned variations in ψ and θ_{2m} make $(\Delta g_{el} + \Delta g_{ch})$ shift to the negative value side. Then, this causes an increase in ρ, as seen from eq. 23 with eqs. 24. As a consequence the accumulation of lipids and proteins occurs so as to produce the excitable membrane, and the transition from the depolarized to resting state takes place. In this state, the present calculation gives $\rho \approx 0.8$, $\rho/\rho_m \approx 0.8$, and hence the dps is about 0.2. Therefore, phase separation exists between Ca^{2+}-rich membranous domains containing tightly packed adsorbed molecules and Ca^{2+}-depleted domains composed of sparsely distributed molecules. Since monovalent cations like Na^+ and K^+ reduce the binding of Ca^{2+} to lipids and proteins on the surface, the increase in Na^+ or K^+ concentration reduces the changeable bridging energy given by eq. 16c. Thus, the occurrence of the phase transition from the depolarized to resting state requires higher Ca^{2+} concentration for higher Na^+ or K^+ concentration, as shown quantitatively in fig. 4. The present theory can explain the observed antagonistic tendency of monovalent cations and Ca^{2+} for the appearance of the excitable membrane. (cf. fig. 2d.)

Further increase in Na^+ (or K^+) or Ca^{2+} concentration in the resting state, however, destabilizes the state of phase separation. In the present calculation, $\rho \approx 0.05$, $\rho/\rho_m \approx 1$ and dps ≈ 0 are obtained under this condition. It is concluded, therefore, that most of molecules adsorbed on the surface cannot form a membrane structure, and return to the interior of the droplet. Consequently, the phase transition occurs from the resting state to the depolarized state as Na^+ and Ca^{2+} concentrations are increased. In the depolarized state observed at higher ion concentrations, adsorbed molecules may distribute very sparsely but homogeneously. The situation is illustrated in fig. 2a.

3. Dynamic properties of accumulation of membrane-constituting molecules

3.1. A theoretical model

In the preceding section, the ion concentration in the inner surface region was assumed to be equal to the external one. However, the original ion concentration will be restored once the excitable membrane has been formed. A large ion-concentration gradient is maintained across the membrane in the resting state, while it can scarcely exist in the depolarized state. This demonstrates the gradual change in the ion concentration in this region during the membrane-forming process. Thus, we must relax the restriction concerned with the ion concentration when discussing kinetics of membrane formation. Fig. 5 illustrates these situations, where the ion concentration in the inner surface region is different from the external one. In fig. 5, the transitional region between the central and inner surface regions is neglected; we approximate the ion concentration in each region as uniform. Within the frame of this approximation, we have only to discuss a change in the average ion concentration in the inner surface region instead of investigating a detailed spatial distribution of ion concentrations over the whole region. When the ion concentration in the inner surface region becomes equal to that in the central region, therefore, the inner surface region can be regarded as being absent.

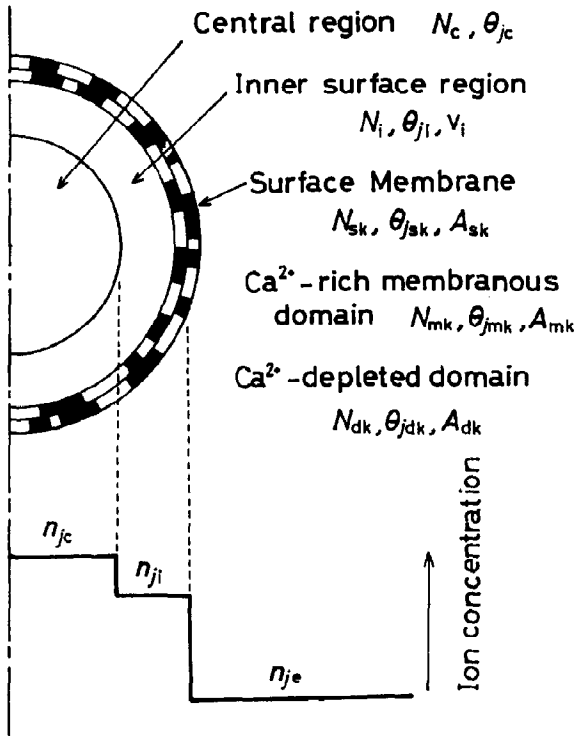

Fig. 5. An improved theoretical model for describing the dynamic properties of membrane formation, as well.

The surface membrane is composed of two interacting adsorbed monolayers in this model. As can be seen from fig. 5, the interior and exterior part of the bilayer touch n_{ji} and n_{je}, respectively, which are usually different from each other. This causes some differences between typical quantities such as the packing density and degree of adsorption of Ca^{2+}. The membrane can be considered as asymmetric with interior and exterior parts. Therefore, we must distinguish clearly the interior monolayer from the exterior monolayer, fig. 5 also shows this situation. N_c, N_i, N_{sk}, N_{mk}, N_{dk}, number of lipids and proteins; θ_{jc}, θ_{ji}, θ_{jsk}, θ_{jmk}, θ_{jdk} degree of adsorption of j-th cations on lipids and proteins; A_{sk}, A_{mk}, A_{dk}, surface area; n_{jc}, n_{ji}, n_{je}, concentration of jth cations; where the quantities defined at the membrane have the supplementary subscripts k = i and e for denoting the interior and exterior parts of bilayer, respectively.

The controllable parameters are the external ion concentrations n_{je}.

In the present section the following approximations may also be useful for reducing the number of internal variables investigated explicitly:

(i) The total number of lipids and proteins contained in the surface membrane and inner surface region remains constant. The number of adsorbed molecules N_{mk} in the Ca^{2+}-rich membranous domain is much larger than N_{dk} (≈ 0) in the Ca^{2+}-depleted domain.

(ii) In the adsorption of cations on lipids and proteins, monovalent cations like Na^+ and K^+ as well as divalent cations such as Mg^{2+} are scarcely bound to lipids and proteins with a mono-negatively charged group.

(iii) The surface area A_{mk} of the Ca^{2+}-rich membranous domain can be related explicitly to the number of adsorbed molecules N_{sk} and mono- and divalent cation concentrations.

Besides the above approximations, let us make an additional simplification:

(iv) In the surface membrane, the number of molecules contained in the interior monolayer is equal to that in the exterior monolayer. This approximation does hold true for liposomes with a small diameter but is valid for the present large droplet with a diameter ranging from 200 to 400 μm. Thus, the total number simply amounts to $2N_s$ at the effective surface area $2A_s$ with N_s denoting N_{si} ($= N_{se}$) and A_s denoting A_{si} ($= A_{se}$). In spite of this condition, such quantities as the packing density of Ca^{2+}-rich membranous domains and the degree of adsorption of Ca^{2+} can differ in the interior and exterior monolayers. Therefore, the membrane can be asymmetric.

The depolarized and resting states can be characterized by lower and higher packing densities, respectively, of adsorbed molecules in the surface membrane. To describe these states, the packing density averaged over the surface membrane is introduced by eq. 10. On the other hand, the packing density in Ca^{2+}-rich membranous domains in each monolayer is defined as

$$\rho_{mk} = N_{mk} a / A_{mk} \quad \text{for k = i,e,} \tag{27}$$

where the subscripts i and e denote the interior and exterior parts of bilayer at the surface, respectively. By the use of the above approximations (i) and (iii), N_{mk} becomes equal to N_s, and ρ_{mk} is given by

$$\rho_{mk} = \rho / u_k \quad \text{for k = i, e,} \tag{28}$$

where u_k has the following functional form:

$$u_k = A_{mk}/A_s = 1 - (1 - \rho^r)\exp[-q(n_{1k} + 3n_{2k})] \quad \text{for k = i,e.} \tag{29}$$

Eqs. 27, 28 and 29 correspond to eqs. 12, 15 and 14, respectively.

3.2. Free energy

The total free energy of the system is given by eq. 7. According to eq. 16a, the nonelectric part of free energy for the adsorbed bilayer can be rewritten as:

$$F_0 = N_s \sum_{k=i,e} \left\{ \left(-\epsilon_0 + \frac{\epsilon_r}{\gamma+1}\rho_{mk}^{\gamma} - \frac{\epsilon_a}{\gamma'+1}\rho_{mk}^{\gamma'} - \frac{\epsilon_b}{2}\rho_{mk} \right) + \ln\left[\frac{N_s}{\Delta l (A_{mk} - N_s a)} \right] \right\} + (N - 2N_s)\ln\left[\frac{N - 2N_s}{v_i} \right]. \tag{30a}$$

The electrochemical part F_{el} is also obtained from eq. 16b:

$$F_{el} = N_s \sum_{k=i,e} \left\{ \int_{1/2}^{\theta_{2mk}} \ln\left[\frac{1}{K_2 n_{2k}} \cdot \frac{2\theta}{1-2\theta} \right] d\theta + \left(\frac{a}{\rho_{mk} k_B T} \right) \int_0^{\sigma_k} \psi_k(\sigma) d\sigma \right\} + (N - 2N_s) \int_{1/2}^{\theta_{2i}} \ln\left[\frac{1}{K_2 n_{2i}} \cdot \frac{2\theta}{1-2\theta} \right] d\theta. \tag{30b}$$

The surface charge density σ_k is given by

$$\sigma_k = -(e\rho/a u_k)(1 - 2\theta_{2mk}) \quad \text{for k = i,e,} \tag{31}$$

and

$$\sigma_k = \sqrt{2\epsilon_W k_B T/\pi} \times \sinh(\phi_k/2)\left[n_{1k} + n_{2k}(e^{-\phi_k} + 2) \right]^{1/2} \quad \text{for k = i,e.} \tag{32}$$

The reduced electrostatic potential at the surface ϕ_k is defined by

$$\phi_k = e\psi_k/k_BT \quad \text{for k = i,e.} \tag{33}$$

The term E_{ch} expressing the bridging ability of Ca^{2+} is rewritten as;

$$E_{ch} = -N_s\epsilon_2 \sum_{k=i,e} \theta_{2mk}^2\sqrt{\rho_{mk}}\,. \tag{30c}$$

The boundary energy E_b of eq. 16d is reduced to

$$E_b = N_s\bar{\epsilon}_b \sum_{k=i,e} \lambda_k^{-2}/\sqrt{u_k}\,, \tag{30d}$$

where the normalized and modified screening length λ_k is defined by

$$\lambda_k{}^2 = 1 + (8\pi e^2/\epsilon_W k_BT)a(n_{1k} + 3n_{2k}) \quad \text{for k = i,e.} \tag{34}$$

3.3. Accumulation kinetics of membrane-constituting molecules

3.3.1. Kinetic equation for ρ

For describing the dynamic behavior of membrane formation, let us assume the following kinetic equation of the Ginzburg-Landau type [14] for ρ:

$$\tau\frac{d\rho}{dt} = -\frac{\partial F}{\partial \rho}\,, \tag{35}$$

where τ is the time factor for expressing the damping. The right-hand side of eq. 35 is given by

$$\frac{a}{2A_s}\frac{\partial F}{\partial \rho} = \Delta g = \Delta g_0 + \Delta g_{el} + \Delta g_{ch} + \Delta g_b; \tag{36}$$

$$\begin{aligned}\Delta g_0 = &-(\epsilon_0 + \ln c)\\ &+(1/2)\sum_{k=i,e}\Big\{\Big[\epsilon_r(\rho/u_k)^{\gamma} - \epsilon_a(\rho/u_k)^{\gamma'}\\ &-\epsilon_b(\rho/u_k)\Big] - \ln\{\Delta la[(u_k/\rho)-1]\}\Big\}\\ &+(1-P_k)/[(u_k/\rho)-1]\\ &-P_k\Big[\frac{\gamma}{\gamma+1}\epsilon_r(\rho/u_k)^{\gamma+1}\\ &-\frac{\gamma'}{\gamma'+1}\epsilon_a(\rho/u_k)^{\gamma'+1}\\ &-\frac{\epsilon_b}{2}(\rho/u_k)^2\Big]\Big\},\end{aligned} \tag{37a}$$

$$\begin{aligned}\Delta g_{el} + \Delta g_{ch} = &-\ln\sqrt{\theta_{2i}}\\ &+(1/2)\sum_{k=i,e}\Big\{\ln\sqrt{\theta_{2mk}}\\ &-P_k a\Pi_{el,k}/k_BT\\ &-\epsilon_2\theta_{2mk}(1-\theta_{2mk}/2)\sqrt{\rho/u_k}\\ &+(P_k/2)\epsilon_2\theta_{2mk}^2(\rho/u_k)^{3/2}\Big\},\end{aligned} \tag{37b}$$

$$\Delta g_b = (\bar{\epsilon}_b/2)\sum_{k=i,e}\lambda_k^{-2}[1-(P_k/2)(\rho/u_k)]/\sqrt{u_k}\,, \tag{37c}$$

where c is given by eq. 25 and P_k is similar to eq. 26 replaced with n_{1k} and n_{2k} for k = i and e. The electrostatic pressure is denoted by $\Pi_{el,k}$ as a function of n_{1k}, n_{2k} and ϕ_k. The function u_k for describing the phase separation is given by eq. 29 as a function of ρ, n_{ik} and n_{2k}.

3.3.2. Adsorption equilibrium

As for the degrees of adsorption θ_{2i}, θ_{2mi} and θ_{2me}, we can consider a steady state because of a rapid interaction between cations and molecules of lipids and proteins compared with diffusion of these molecules to the surface. Since the ion concentration in the inner surface region changes slowly with membrane formation, the degrees of adsorption also change slowly; the above steady-state consideration involves the elimination of a fast relaxational component. Thus, the minimization of F with respect to θ_{2i}, θ_{2mi} and θ_{2me} gives

$$1 - 2\theta_{2i} = (1 + K_2 n_{2i})^{-1}, \tag{38}$$

$$1 - 2\theta_{2mk} = \Big\{1 + K_2 n_{2k} \times \exp\Big[-2\phi_k + 2\epsilon_2\theta_{2mk}\sqrt{\rho/u_k}\Big]\Big\}^{-1} \quad \text{for k = i,e.} \tag{39}$$

If the ion concentrations n_{1i} and n_{2i} in the inner surface region given later are substituted into eqs. 35, 38 and 39 with eqs. 37, we can describe in

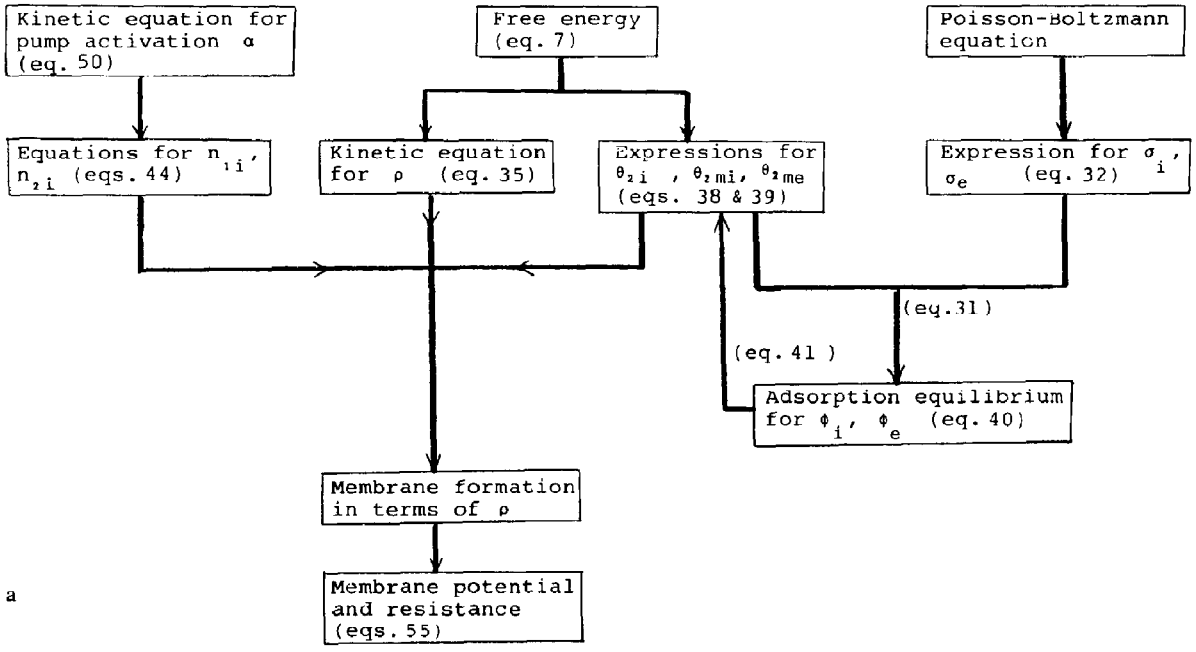

a

Fig. 6. Procedures for membrane formation. (a) Original procedure and (b) the present procedure using the approximate expression (eq. 43).

principle the accumulation of membrane-constituting molecules at the surface after the external solution is replaced by the testing solution. The detailed procedure is as follows: the degree of adsorption θ_{2i} is given directly by eq. 38, but θ_{2mk} may first be obtained if the surface potential ϕ_k can be calculated by the adsorption equilibrium obtained from eqs. 31, 32 and 39. For the adsorption equilibrium we obtain

$$-(e\rho/au_k)\left\{1+K_2n_{2k}\times\exp\left[-2\phi_k+2\epsilon_2\theta_{2mk}\sqrt{\rho/u_k}\right]\right\}^{-1} = \sqrt{2\epsilon_W k_B T/\pi}\,\sinh(\phi_k/2)\times\left[n_{1k}+n_{2k}(e^{-\phi_k}+2)\right]^{1/2} \quad \text{for k = i,e.} \tag{40}$$

If the right-hand side of eq. 40 is denoted by I, θ_{2mk} is given by

$$2\theta_{2mk} = 1+(au_k/e\rho)I \quad \text{for k = i,e.} \tag{41}$$

The value of ϕ_k can be calculated only numerically for given values of n_{1k} and n_{2k}. Fig. 6a summarizes the procedure for describing the membrane formation. As can be seen from fig. 6a, the electrochemical description of membrane formation seems very complicated owing to the interference of the adsorption equilibrium of eq. 40. However, if we can obtain an approximate but analytic expression for ϕ_k, the kinetic equation for ρ will be reduced to a more simplified equation by eliminating θ_{2mk} with eq. 39 or 41.

For this purpose, we neglect the term proportional to ϵ_2 caused by the bridging in eq. 40. Since this term reaches about 30% of the value of the term $-2\phi_k$ when θ_{2mk} and ρ are increased, this approximation does not always give a satisfactory result. moreover, the present situation is concerned with Ca^{2+} concentrations as low as a few multimolar in the basal and testing solutions. This omission therefore becomes a fairly good approximation for the present purpose; in fact it will be demonstrated later. Eq. 39 for θ_{2mk} can be

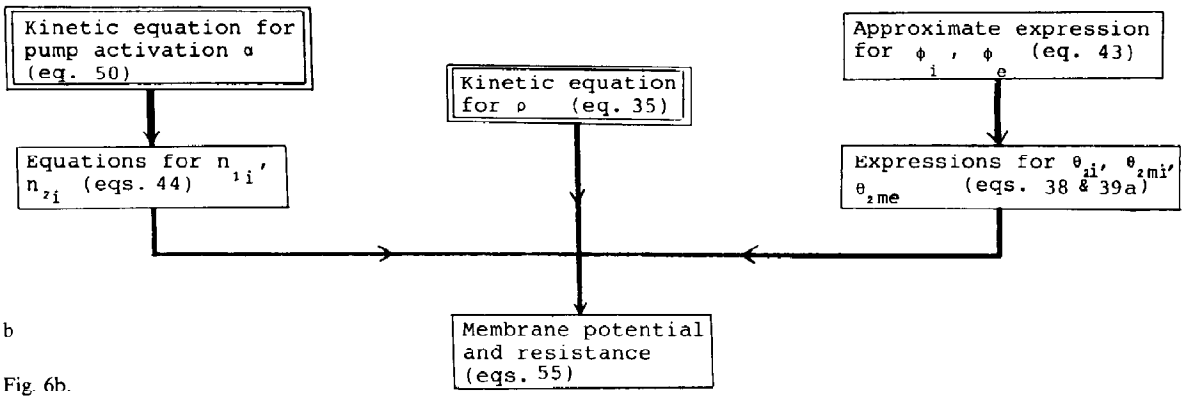

b

Fig. 6b.

approximated by

$$1 - 2\theta_{2mk} = \left[1 + K_2 n_{2k} \exp(-2\phi_k)\right]^{-1} \quad \text{for k = i,e.} \tag{39a}$$

In the second place, we consider the following situation:

$$\exp(-\phi_k) \gg 1, \ (n_{1k}/n_{2k}) \exp(\phi_k) \ll 1 \quad \text{for k = i,e.} \tag{42}$$

This may apply to a high-potential approximation [6], which is also used in the derivation of an analytic expression for the surface potential in the case of proton dissociation [7].

With the aid of these two approximations in eq. 40, we readily obtain:

$$\exp(-\phi_k) \approx \left(2\pi e^2/\epsilon_W k_B T\right)^{1/6} \times (\rho/aK_2 u_k)^{1/3}/\sqrt{n_{2k}} \quad \text{for k = i,e.} \tag{43}$$

By putting this result into eq. 39a, the degree of adsorption θ_{2mk} can be expressed by ρ, n_{1k} and n_{2k}. The kinetic equation for ρ therefore contains only three internal variables, ρ, n_{1i} and n_{2i}, although eight variables, ρ, n_{1i}, n_{2i}, ϕ_i, ϕ_e, θ_{2i}, θ_{2mi} and θ_{2me}, were included formally in the original expressions.

The present scheme using the approximate expressions for ϕ_i and ϕ_e is summarized in fig. 6b. The process of membrane formation can be described by two kinetic equations for the packing density ρ and the pump activation α, mentioned below, through the degrees of adsorption and the internal ion concentrations.

4. Change in ion concentration in inner surface region with activation of pump

When the external solution is exchanged with the testing solution, the ion concentration in the droplet near the surface decreases as shown in fig. 5. The subsequent membrane formation will result in pump activation which restores the original ion concentration. A remarkable difference between the ion concentrations of basal and testing solutions is that the monovalent cation concentration is represented by a ratio of about 100 : 1. The membrane formation can be considered as being attributed mainly to the change from high to very low monovalent cation concentrations. We therefore focus the present description on the change concerned with monovalent cations. As for divalent cations such as Ca^{2+}, the concentration in the inner surface region is assumed to be equal to the external one, in a similar way to that described in section 2. This is partly because the high-potential approximation of eq. 42 is no larger valid for such low concentrations as 0.1 μM reported in Characean cells [15].

$$n_{2i} = n_{2e}. \tag{44a}$$

Furthermore, anions like Cl^- are assumed to redistribute on the macroscopic spatial scale according

to an electrical neutrality accompanied by changes in cation concentrations.

Let us give explicit expressions for the passive and active fluxes. It may reasonable to assume a linear relation between the passive flux J_p and the ion concentration difference Δn:

$$J_p = p\Delta n, \tag{45}$$

with Δn defined by

$$\Delta n = n_{1i} - n_{1e}, \tag{46}$$

where p is the membrane permeability of the monovalent ions and the sign of the flux is taken as positive for efflux. The membrane permeability can be supposed to be a decreasing function of the packing density ρ. Hence, it may be convenient to adopt the following form:

$$p = p^0(\rho^0 - \rho), \tag{47}$$

where p^0 and ρ^0 are the numerical parameters.

As for the active flux J_a, a reliable functional form cannot be anticipated at present owing to a lack of any definite information on the biophysical characteristics of pump molecules. It may now be in order to consider a decreasing feature with increased Δn because a pump works for the maintenance of the ion concentration gradient across the membrane. By also taking into account the convenience of the mathematical procedure, we adopt a simple form (see fig. 7):

$$J_a = \begin{cases} -\alpha(\Delta n_t - \Delta n) & \text{for } \Delta n < \Delta n_t, \\ 0 & \text{for } \Delta n > \Delta n_t, \end{cases} \tag{48}$$

where α is the activation factor described in detail below, and Δn_t is the threshold value of the ion concentration difference beyond which the pump stops. We consider the situation $\Delta n < \Delta n_t$ as a possibly interesting case. A functional form qualitatively similar to eq. 48 is proposed for discussing the behavior of a reaction-diffusion system [16].

Within the present scheme shown in fig. 5, where a uniform ion concentration is supposed to exist in each region, the passive flux may be considered to balance the active flux. This is illustrated in fig. 7. We thus obtain

$$J_p + J_a = 0. \tag{49}$$

This equation is consistent with the situation where the diffusion of ions is much faster than that of membrane-constituting molecules. Eq. 49 with eqs. 45–48 gives the expression for n_{1i}:

$$n_{1i} = n_{1e} + \frac{\alpha}{\alpha + p^0(\rho^0 - \rho)}\Delta n_t. \tag{44b}$$

We now give a kinetic equation for pump activation. Activation is assumed to obey the simple equation given by

$$\frac{d\alpha}{dt} = k_a(1 - \alpha) - k'_a\alpha, \tag{50}$$

where k_a and k'_a are the relevant rate constants. Since lipoprotein complexes are formed on membrane formation, the rate constant k_a can be reasonably considered as being proportional to the packing density:

$$k_a = k_a^0\rho, \tag{51}$$

with k_a^0 denoting the numerical coefficient.

Eq. 50 with eq. 51 describes the pump activation coupled with kinetics of ρ expressed by eqs. 35, 36, 37 and 43 through n_{ji} of eqs. 44 (see fig. 6b).

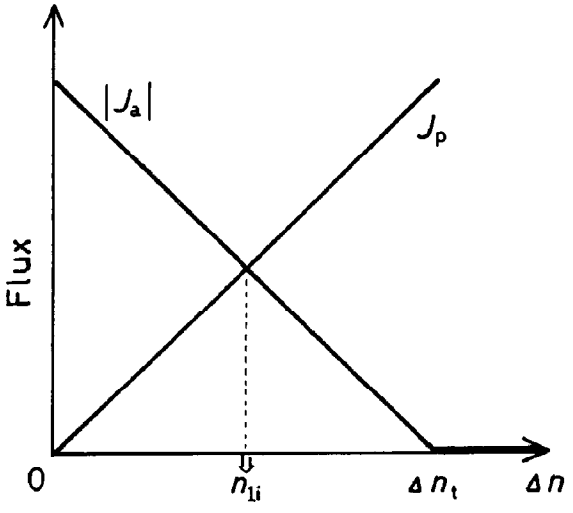

Fig. 7. Active flux and passive flux. Since a steady flux is assumed, the ion concentration n_{1i} can be readily given by the intersection of $|J_a|$ and J_p.

5. Effects of a chemical substance interacting strongly with membrane-constituting molecules

Ion species such as UO_2^{2+} with a strong binding ability to phospholipids can induce periodic changes in the membrane potential and the membrane resistance presumably accompanied by disruption and construction of a membrane [1,4]. In this section, kinetic equations for describing the effects of these kinds of chemical substances on membrane formation are derived.

Let x be the concentration of chemical substance near the droplet, then an equation of the reaction-diffusion type can be written as

$$\frac{dx}{dt} = D(X - x) - k_+ \rho, \tag{52}$$

where D corresponds to the diffusion constant, X is the steady concentration and k_+ the rate constant. The first term in eq. 52 represents diffusion of chemical substance. The second expresses the loss of these species caused by the binding to membrane-constituting molecules, which may be supposed to be roughly proportional to the packing density.

The kinetic equation for ρ of eq. 35 must be altered so that the effect of these ions on the membrane can be described. It can be written as

$$\frac{a\tau}{2A_s} \cdot \frac{d\rho}{dt} = -\Delta g + k'_+ x - \beta, \tag{53}$$

with the numerical constants k'_+ and β. The first term Δg in eq. 53 is given explicitly by eqs. 36 and 37a–37c. The second term expresses the enhancement of the packing density originating from the strong binding of these ions to membrane-constituting molecules followed by rapid aggregation. The final term represents the escape of membrane-constituting molecules aggregated by these ions from the surface.

The strength of binding between these ions and adsorbed molecules may be regarded as being expressed by k_+, k'_+ and β. We can quite reasonably adopt the following relation:

$$\beta = dk_+, \quad k'_+ = d'k_+, \tag{54}$$

where d and d' are the appropriate numerical coefficients. The stronger the binding becomes, the larger k_+ may be expected to be. A set of equations for investigating the effect of chemical substances on membrane formation is composed of eq. 53 for ρ with Δg of eqs. 37 through eqs. 44 giving $n_{ji}(j = 1, 2)$, eq. 50 for the pump activation and eq. 52 for the chemical substance.

6. Comparison with observed data

The membrane potential and membrane resistance are typical quantities reflecting the conformational state of the surface membrane of the *Nitella* protoplasmic droplet [1,4].

We adopt the membrane potential V as follows [17]:

$$V = 59.2 \log \frac{[K^+]_e + P_m[Na^+]_e}{[K^+]_i + P_m[Na^+]_i}, \tag{55a}$$

where the numerical coefficient is evaluated at 25°C. The K^+ and Na^+ concentrations are denoted by $[K^+]_e$, $[K^+]_i$ and $[Na^+]_e$, $[Na^+]_i$, respectively (subscripts: e, external; i, internal). The ratio of the membrane permeability concerned is P_m. The difference between ion species such as K^+ and Na^+ has little effect on the phase transition between the depolarized and resting states, and also on the membrane-forming process [1].

For this reason, the present theory does not distinguish K^+ from Na^+ explicitly, except for assuming a proportional relation between $[K^+]_i$ and $[Na^+]_i$ given by

$$[Na^+]_i / [K^+]_i = \delta. \tag{56}$$

The ratio δ is determined from experiment, and usually lies between 0.03 and 0.1 [17]. The sum is equal to n_{1i}:

$$[K^+]_i + [Na^+]_i = n_{1i}. \tag{57}$$

Eqs. 56 and 57 can give $[K^+]_i$ and $[Na^+]_i$; hence, the membrane potential V can be calculated only if n_{1i} and P_m are given under the externally controllable parameters of $[K^+]_e$ and $[Na^+]_e$ the sum of which is equal to n_{1e}.

The value of P_m is of the order of 0.1 under normal conditions in Characean algae [17]. It implies a much higher permeability to K^+ than Na^+.

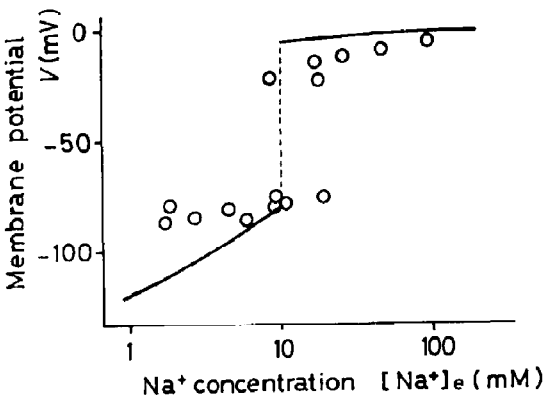

Fig. 8. Theoretical result of steady-state characteristics. The ionic composition other than Na^+ is fixed at 0.5 mM KNO_3, 1 mM $Ca(NO_3)_2$ and 2 mM $Mg(NO_3)_2$. Experimental data [1] are shown by open circles. Numerical parameters: $\epsilon_0 + \ln c = 10$, $\delta = 0.05$, $\hat{d} = 0.1$, $\Delta n_t = 121$ (mM), $p^0 = 0.0135$ (cm/h), $k_a^0 = 0.0108$ (h^{-1}), $k_a' = 1.08$ and $\rho^0 = 1$. Other parameters are the same as fig. 4.

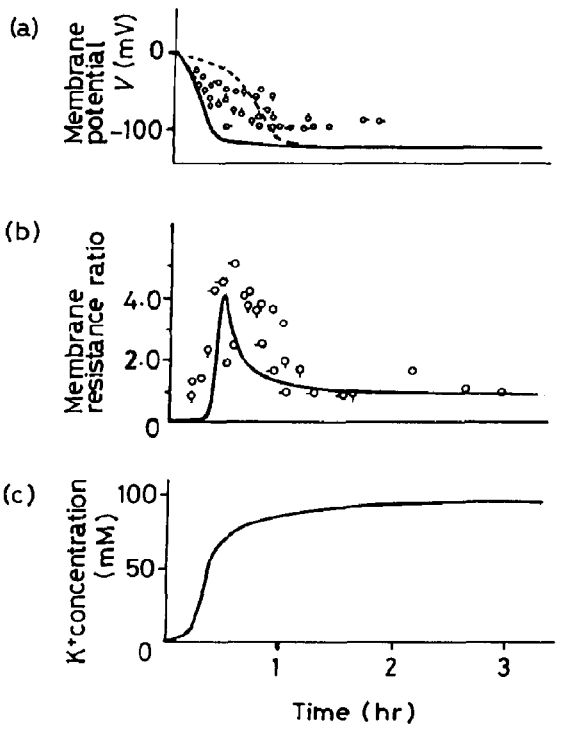

Fig. 9. Membrane formation after the external solution is replaced from the basal solution to the testing solution at $t = 0$. Different symbols refer to different drop specimens [1]. Thick solid lines are obtained with the same parameter values as in fig. 5 except $\epsilon_0 + \ln c = 13.5$, $a\tau/2A_s = 2$ (h), $R_0 = 10$ (k$\Omega \cdot cm^2$) and $\rho^* = 0.879$. The dashed line expresses an example of dynamic metastability by choosing $\epsilon_0 + \ln c = 12.45$. The initial values of ρ and α are given by eqs. 11 and 28, respectively, with $d/dt = 0$ under the condition of basal solution: $\rho = 0.059$, $\alpha = 5.9 \times 10^{-4}$ (approximated by zero). The initial K^+ concentration in the inner surface region is determined from eqs. 22b, 34 and 35 using the above values of ρ and α, and is equal to 0.95 mM in the testing solution.

However, the large difference between the permeabilities of these ions must disappear when the surface membrane is not formed. Therefore, we can assume that P_m depends only on the packing density ρ. It is convenient to adopt the following linear form:

$$P_m = 1 - (1 - \hat{d})\rho, \tag{58}$$

where $\hat{d}$ is a numerical constant with a value of about 0.1. For ρ equal to unity P_m becomes $\hat{d}$, and P_m approaches unity as ρ is decreased to zero.

As for the membrane resistance R, we assume a simple relation given by

$$R = \frac{R_0}{\rho^* - \rho}, \tag{55b}$$

with R_0 and ρ^* indicating numerical parameters. Eq. 55b expresses the natural relationship between the resistance and the packing density: R becomes larger with the accumulation of membrane-constituting molecules. The value of ρ^* is taken as slightly larger than the maximum value of ρ obtained by the present calculation for ρ.

The membrane potential V in eq. 55a and the membrane resistance R in eq. 55b can be calculated if ρ and n_{1i} are known from eq. 35 and eq. 44b, respectively.

The theoretical result for the steady-state characteristics is shown in fig. 8. The observed tendency for the change in Na^+ concentration is explained fairly well in spite of the present simplified approximation of eq. 43 in obtaining the solution for ϕ_i and ϕ_e. This fact may lend support to the present approximation.

Fig. 9 shows plots of the calculated kinetics of

the membrane potential, membrane resistance and K^+ concentration in the inner surface region after the external solution was exchanged with the testing solution from the basal solution. The monotonic decrease in the membrane potential V as well as the temporal increase in the membrane resistance R are described well. The recovery of ion concentration in the inner surface region, which was close to the external ion concentration at the first stage, is also shown in fig. 9c.

This feature can be understood by considering theoretical results and physicochemical experiments [1]: A gradual activation of pump molecules resulting from the accumulation of membrane-constituting molecules at the surface, followed by the rearrangement to form lipid-protein complexes, produces the gentle change in ion concentration within the droplet and the monotonic decrease in V. The rapid temporal increase in R may be caused by the accumulation of lipids at the surface. The subsequent slow decrease is due to the penetration of proteins into the lipid membrane [1,2]. This is reflected rather indirectly by the calculated result that the packing density increases transitionally to $\rho = 0.875$ from $\rho = 0.059$ but then decreases only slightly to $\rho = 0.862$, which leads to the change in R of eq. 55b. The small reduction of ρ is brought about by the increased ion concentration in the inner surface region arising from pump activation. While our theoretical model may be inadequate for discussing more detailed conformational change owing to the average treatment of molecular species such as lipids and proteins, the observed characteristic kinetics of the membrane potential and resistance can be explained well.

An apparently curious change in the membrane potential accompanied by the time delay to reach the final value can be obtained by choosing adequately the value of the parameter $(\epsilon_0 + \ln c)$. An example of the theoretical results is also shown in fig. 9a. This type of time course has been observed experimentally for some samples [1]. Somewhat qualitative features can be discussed using the present theory: The adsorption process of lipids and proteins at the surface is well known to be a first-order phase transition [10]. It has been shown experimentally and theoretically that a dynamic

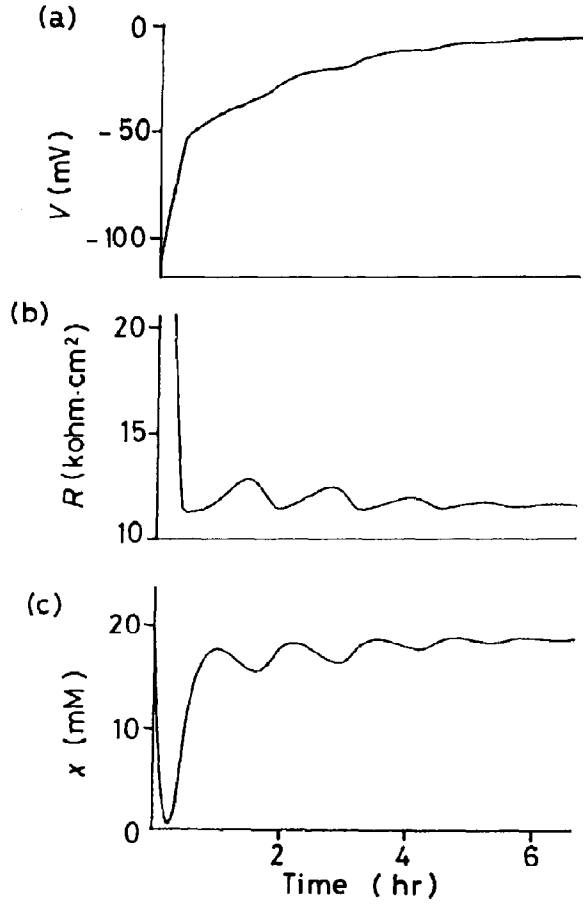

Fig. 10. Oscillations in the presence of interacting strongly with the membrane. Parameters: $p^0 = 0.121$, $X = 20$ (mM), $D = 4.5$ (h^{-1}), $k = 11.13$ (mM/h), $d = 17.14$ (h/mM) and $d' = 0.0476$ (h/mM^2). The other parameters are chosen as in fig. 6.

metastability appears in the first-order phase transition or some similar phase transitions with the dominant nucleation process concerned [18–21]. In the system considered now, the conformational state characterized by the lower packing density is also stable or located near the stability point. Thus, the system stays there for a while, but afterwards it will pass into another state with a higher packing density showing the larger magnitude of V, which is more stable in the thermodynamic sense.

Fig. 10a and b demonstrates calculated exam-

ples of periodic changes in V and R for a droplet in the testing solution containing a chemical substance interacting strongly with membrane-constituting molecules. As observed experimentally in the presence of UO_2^{2+} [4], the membrane becomes depolarized gradually while showing periodic variations of the membrane potential and membrane resistance. The time course of the concentration of chemical substance x is shown in fig. 10c. These changes reflect the competitive formation and disruption of the membrane caused by the strong binding of UO_2^{2+} to phospholipids.

Furthermore, the rapid depolarization without periodic changes could also be obtained numerically by increasing the value of parameter k_+ in eq. 54. This result resembles an experimental observation made in the application of an SH reagent such as *p*-chloromercuribenzoate to the droplet [22].

In this way, the membrane can be considered essentially as a dynamic ordered structure maintained far from equilibrium in the open system dominated mainly by the electrochemical process, where membrane-constituting molecules move into the surface structure and are sometimes released from the surface, as suggested by Kobatake et al. [1].

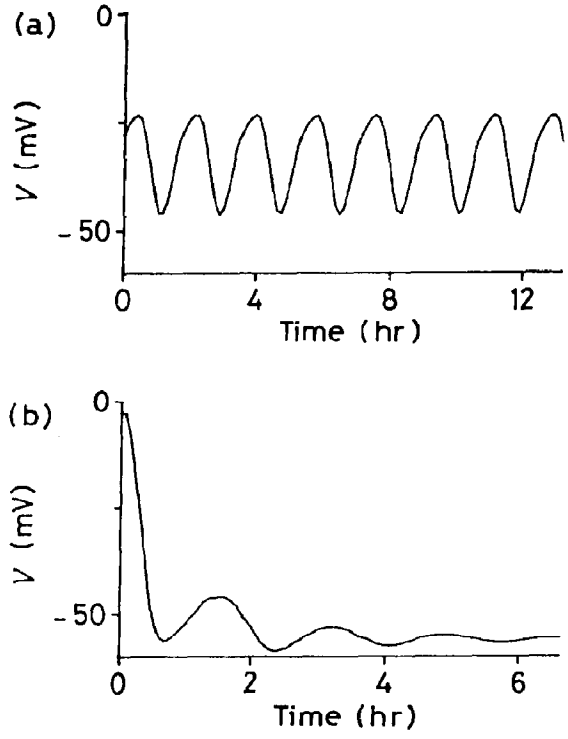

Fig. 11. Examples of self-sustained oscillations (a) and oscillations during the membrane-forming process (b). Parameters: (a) $k_+ = 9.45$, (b) $k_+ = 8.4$.

7. Discussion

Periodic changes in membrane potential or surface potential have often been observed in growth and regeneration processes in biological systems such as root elongation in beans [23] and cap formation in the unicellular alga *Acetabularia* [24]. While a causal relationship between self-oscillations and growth has not yet been established, it is reasonable to suppose that the membrane-forming process plays a fundamental role in growth from the viewpoint of electrochemical origins under nonequilibrium conditions. In fact, the regeneration process in *Acetabularia* depends strongly on the Ca^{2+} concentration in the external media. The experimental result that much lower as well as higher Ca^{2+} concentrations prohibit cap formation [25] is quite analogous to the observation in the *Nitella* protoplasmic droplet [1].

Fig. 11a shows an example of self-sustained oscillations given by eq. 53 for ρ, eqs. 44 for n_{ji} ($j = 1, 2$), eq. 50 for α and eq. 52 for x, which appeared by choosing a somewhat smaller value of k_+ than for the case in fig. 10. A damped oscillation in membrane formation after replacement of the external solution by the testing solution is shown in fig. 11b. A build-up of the membrane potential exhibiting oscillations can be seen. It may describe relatively well an oscillation observed in the droplet [26]. In the experiment, however, UO_2^{2+} was not included. Since Ca^{2+} bridges between lipids [3,5] with an affinity even weaker than that of UO_2^{2+}, the possibility may exist that the oscillatory transition induced by the Ca^{2+} bridging is accompanied by spatial local changes in packing density. In the present theory, a quasi-stationary state is assumed for Ca^{2+}-bridging kinetics in eqs. 38 and 39. To explain more pre-

cisely the oscillation induced by Ca^{2+} bridging, therefore, the kinetics of Ca^{2+} adsorption to lipids and proteins must be taken into account.

These numerical examples may help us to confirm the impression of the drastic dynamic properties of the membrane structure maintained under far-from-equilibrium conditions. However, basic physicochemical data are lacking for the understanding of a mechanism of oscillations in individual systems such as *Acetabularia* and bean roots. Although the direct application of a simple theory such as that studied here to these phenomena may not yet be available, a comprehensive explanation of a crucial role palyed by self-sustained oscillations in growth might become possible in the near future on the basis of electrochemical theories taking into account the nonequilibrium situation.

References

1 Y. Kobatake, I. Inoue and T. Ueda, Adv. Biophys. 7 (1975) 43.
2 Y. Aizawa and Y. Kobatake, J. Theor. Biol. 60 (1976) 393.
3 K. Toko and K. Yamafuji, J. Theor. Biol. 99 (1982) 461.
4 T. Ueda, M. Muratsugu and Y. Kobatake, Biochim. Biophys. Acta 373 (1974) 286.
5 K. Toko and K. Yamafuji, Biophys. Chem. 14 (1981) 11.
6 H. Träuble, M. Teubner, P. Woolley and H. Eibl, Biophys. Chem. 4 (1976) 319.
7 K. Toko and K. Yamafuji, Chem. Phys. Lipids 26 (1980) 79.
8 H. Ohshima and T. Mitsui, J. Colloid Interface Sci. 63 (1978) 525.
9 S. Ohnishi and S. Tokutomi, Biological magnetic resonance, eds. L.J. Berliner and J. Reuben (Plenum Press, New York, 1981) Vol. 3, p. 121.
10 Y. Suezaki, J. Theor. Biol. 71 (1978) 279.
11 T.A.J. Payens, Philips Res. Rep. 10 (1955) 425.
12 T.L. Hill, Introduction to statistical thermodynamics (Addison-Wesley, Reading, MA, 1960).
13 J.A. DeSimone, J. Colloid Interface Sci. 67 (1978) 381.
14 H. Haken, Synergetics – An introduction (Springer Verlag, Berlin, 1977) 2nd enlarged ed. (1978) ch. 6.
15 G.P. Findly and A.B. Hope, Aust. J. Biol. Sci. 17 (1964) 400.
16 R. Larter and P. Ortoleva, J. Theor. Biol. 96 (1982) 175.
17 A.B. Hope, Ion transport and membrane (Butterworths, London, 1971).
18 H. Tomita and C. Murakami, Prog. Theor. Phys. 64 (1978) 452.
19 K. Binder, Phys. Rev. 8 (1973) 3423.
20 F. Oosawa and M. Kasai, J. Mol. Biol. 4 (1962) 10.
21 K. Toko, J. Nitta and K. Yamafuji, J. Phys. Soc. Jap. 50 (1981) 1343.
22 I. Inoue, N. Ishida and Y. Kobatake, Biochim. Biophys. Acta 367 (1974) 24.
23 B.I.H. Scott, Ann. N. Y. Acad. Sci. 98 (1962) 890.
24 B. Novak, Adv. Chem. Phys. 29 (1975) 281.
25 B.C. Goodwin, J.K. Skelton and S.M. Kirl-Bill, Planta 157 (1983) 1.
26 I. Inoue, T. Ueda and Y. Kobatake, Biochim. Biophys. Acta 298 (1973) 653.